Published in "Developmental Biology 405(2): 202–213, 2015"
which should be cited to refer to this work.

Characterization of *tailless* functions during *Drosophila* optic lobe formation

Oriane Guillermin, Benjamin Perruchoud, Simon G. Sprecher*, Boris Egger*

Department of Biology, University of Fribourg, Chemin du Musée 10, CH-1700 Fribourg, Switzerland

Brain development goes through phases of proliferative growth and differentiation to ensure the formation of correct number and variety of neurons. How and when naïve neuroepithelial cells decide to enter a differentiation pathway remains poorly understood. In the *Drosophila* visual system, four optic ganglia emerge from neuroepithelia of the inner (IPC) and outer (OPC) proliferation centers. Here we demonstrate that the orphan nuclear receptor Tailless (Tll) is a key factor for the development of all optic ganglia. We describe *tll* expression during larval optic lobe development in unprecedented detail and find a spatiotemporally dynamic pattern. In the larval OPC, symmetrically dividing neuroepithelial cells transform into asymmetrically dividing medulla neuroblast and into lamina precursor cells in a precisely regulated fashion. Using genetic manipulations we found that *tll* is required for proper neuroepithelium morphology and neuroepithelial cell survival. We show that *tll* regulates the precise timing of the transition from neuroepithelial cells to medulla neuroblasts. In particular, however, we demonstrate that *tll* has a crucial role for the specification of lamina precursor cells. We propose that the Tll/Tlx transcription factors have an evolutionary conserved role in regulating neural precursor cell states in the *Drosophila* optic lobe and in the mammalian retina.

1. Introduction

Organogenesis can be subdivided in distinct phases of tissue growth, cell type specification and differentiation. Initially during phases of growth stem cells typically proliferate rapidly to expand the pool of undifferentiated precursor cells. These initial growth periods are often characterized by symmetrically dividing stem cells. Later during development progenitor cells enter specific differentiation pathways for the formation of functional organs such as gut, skin or the nervous system. Molecular and genetic mechanisms controlling how and when undifferentiated stem or progenitor cells are assigned to specific cell fate pathways during organ development are not yet resolved.

In *Drosophila* the visual system is composed of the compound eye harboring photoreceptor neurons and an array of optic ganglia, which are required for visual information processing. All these structures arise during embryonic and larval development from two main primordia. The optic lobe of *Drosophila* consists of four distinct ganglia (lamina, medulla, lobula and lobula plate), which are organized in a fashion to allow processing of complex visual information such as colors, motion detection, spatial position and light polarization (reviewed in Sanes and Zipursky, 2010).

During late embryonic stages the optic lobe primordium splits into two neuroepithelia, the outer and the inner proliferation centers (OPC and IPC). Lamina and medulla develop from the OPC that covers the lateral surface of the optic lobe, while lobula and lobula plate derive from the IPC that is positioned deeper inside the optic lobe (Hofbauer and Campos-Ortega, 1990). Previous work suggests that the OPC neuroepithelium is patterned along the mediolateral axis to specify two main progenitor cell pools that generate neurons for medulla and lamina (Hofbauer and Campos-Ortega, 1990). At the medial edge of the OPC symmetrically dividing neuroepithelial cells transition through a sequence of progenitor cell states prior to transforming into asymmetrically dividing medulla neuroblasts (Egger et al., 2007; Yasugi et al., 2008; Yasugi et al., 2010). The lamina arises from the lateral edge of the OPC whereby neuroepithelial cells transform to lamina precursor cells (LPCs) by a mechanism that is not well understood. Incoming photoreceptor neurons convey a Hedgehog (Hh) signal, which triggers a final symmetric division of LPCs to produce pairs of differentiating lamina neurons (Selleck et al., 1992; Huang and Kunes, 1996, 1998). The spatiotemporal specification of medulla neuroblasts and lamina precursor cells from one and the same OPC neuroepithelium is critical to schedule the production of neuronal subtypes in order to build the correct neuronal network, also

* Corresponding authors: Fax: +41 26 300 9741.
E-mail addresses: simon.sprecher@unifr.ch (S.G. Sprecher), boris.egger@unifr.ch (B. Egger).

referred to as retinotopic map. Neurons of the medulla receive input from the retina and the lamina and are organized into columns and layers and project to the lobula and lobula plate (reviewed in Sanes and Zipursky, 2010). The genetic and cellular mechanisms of neurogenesis in the lobula and lobula plate have only recently been explored in greater detail. Distinct types of precursor cells leave the IPC neuroepithelium in migratory streams to reach a new proliferation zone that is positioned centrally underneath the OPC. Two neuronal populations have been described, distal cells and lobula plate neurons that arise from the new proliferation zone (Apitz and Salecker, 2015).

Here we describe a new role for the orphan nuclear receptor Tailless (Tll) in regulating optic ganglia development and in particular in the specification of lamina precursor cells (LPCs). *tll* is expressed in the optic lobe anlagen from early embryonic stages onwards (Rudolph et al., 1997). During embryogenesis *tll* directs cells in the head ectoderm towards an optic lobe cell fate and inhibits an alternative photoreceptor fate (Daniel et al., 1999; Sprecher et al., 2007). A recent report shows that *tll* regulates the transition between two progenitor states in an IPC derived secondary proliferation zone (Apitz and Salecker, 2015). The function of *tll* during larval development in the OPC has not been studied yet.

We found that *tll* shows a dynamic expression pattern during larval optic lobe development. *tll* is expressed at high levels in all neuroepithelial cells of the proliferating OPC and IPC during a phase of optic lobe growth. At later larval stages, *tll* expression is defined by a low and a high expression domain in the OPC neuroepithelium. We show that *tll* knockdown leads to severe growth defects during larval stages that affect all ganglia of the adult optic lobe. One cause of these defects is the role of *tll* in neuroepithelial cell integrity and cell survival. More specific analysis of neuroepithelial precursor formation revealed that at the lateral side of the developing OPC *tll* is required for the correct specification of lamina precursor cells and the production of lamina neurons. On the medulla side we found that *tll* is required for the precise timing of neuroepithelial cell to neuroblast transition. Hence, *tll* is a new factor that is involved in the formation of both major precursor cell types deriving from OPC neuroepithelia, lamina precursor cells and medulla neuroblasts. The study let us conclude that Tll is a key factor in regulating progenitor cell specification and neurogenesis in the developing *Drosophila* visual system.

2. Materials and methods

2.1. Fly stocks

Flies were reared in standard cornmeal medium supplemented with molasses at 25 °C with a 12/12 light cycle. The *tll:EGFP* construct (BL-30874; hereafter called *tll::GFP*) (Venken et al., 2009) was used to visualize the *tll* expression pattern. Besides the expression pattern in the larval brain that we describe in detail below we also detected weak expression in ommatidial cells of the developing eye disk (Fig. S1A and B). We also found that this construct can rescue lethality of tll^{l49} homozygous mutant flies (data not shown). $GAL4^{c855a}$ was used to drive strong expression of UAS constructs in the IPC and OPC from first larval instar onwards (Manseau et al., 1997; Egger et al., 2007). Strong expression is also detected in the peripodial epithelia of the developing eye disk and weak expression is found in individual cells posterior to the morphogenic furrow (Fig. S1C and D). Flip-out clones were induced by the use of *hs-FLP; tub > FRT-cassette > GAL4, UAS-nls.lacZ/CyO Dfd-GFP* (a gift from E. Piddini). Virgin females from both driver lines were crossed with males with the construct *UAS-miRNA.tll* to knockdown *tll* expression or to *UAS-tll* males for *tll* misexpression (gifts from M. Kurusu) (Lin et al., 2009). To inhibit apoptosis in *tll* knockdown clones *hs-FLP; tub > FRT-cassette > GAL4, UAS-nls.lacZ/CyO Dfd-GFP* females were crossed to *UAS-miRNA.tll; UAS-p35* males (BL-5073; Hay et al., 1994). For the control experiments, $GAL4^{c855a}$ virgin females were crossed with *UAS-mCD8::GFP* males and *hs-FLP; tub > FRT-cassette > GAL4, UAS-nls.lacZ/CyO Dfd-GFP* females with *w1118* males. To induce *tll* loss-of-function MARCM (Mosaic Analysis with a Repressible Cell Marker) clones virgin females with genotype *hs-FLP; tub-GAL4, UAS-mCD8-GFP/CyO, act-GFP; FRT82B, tub-GAL80/TM6B* (gift from B. Bello and H. Reichert) were crossed with males of genotype *FRT82B,* tll^{l49}*/TM6B* (gift from M. Kurusu) (Lin et al., 2009) or *UAS-p35; FRT82B,* tll^{l49}*/TM6B* (BL-5072; Hay et al., 1994).

2.2. Staging and clonal induction

For staging, embryos were collected in a 4 h time window on apple juice plates. About 80–100 freshly hatched larvae were collected 24 h after egg laying and transferred onto cornmeal food plates containing a drop of liquid yeast. Larvae were then selected for dissection at appropriate stages 24 h, 48 h, 72 h and 96 h after larval hatching (ALH) and pharate pupae were collected after 10 days. In order to induce Flip-out clones larvae were heat-shocked for 10 min at 37 °C at 12 h or 24 h ALH. Larvae with the correct genotype were selected by the absence of GFP balancer with a fluorescence binocular. Brains were dissected at 48 h or 72 h ALH, respectively. To induce MARCM clones larvae were heat-shocked for 30 min at 37 °C at 24 h ALH and dissected at 72 h ALH.

2.3. Immunofluorescence labeling

Immunofluorescence stainings were done as described in (Perruchoud and Egger, 2014) with minor modifications. Briefly, at the desired larval or pharate adult stage brains and eye disks were dissected in 1 × PBS and fixed in 4% Formaldehyde (Sigma Aldrich), 1 × PBS with 5 mM $MgCl_2$, 0.5 mM EGTA for 18 min at room temperature. Brains were rinsed 3 times 15 min with 1 × PBS with 0.3% Triton X100 (PBST) (Sigma Aldrich) at room temperature. Brains were then incubated with primary antibodies in PBST overnight at 4 °C. The next day, brains were rinsed 3 times 30 min in PBST before incubation with secondary antibodies overnight at 4 °C. Brains were again washed 3 times 30 min in PBST and incubated in Vectashield (VectorLabs) with or without DAPI overnight at 4 °C. Finally, brains were mounted in Vectashield on a microscopy slide prior to confocal imaging. The following primary antibodies were used: mouse anti-Dlg (4F3, 1:25), rat anti-DECad (DCAD2, 1:20), mouse anti-Dac2-3 (mAbDac2-3, 1:50), mouse anti-FasII (1D4, 1:20), all from DSHB, Guinea pig anti-Dpn (1:1000) (a gift from J. Skeath), Guinea pig anti-Dpn (1:5000) and rat anti-L'sc (1:5000) (gifts from A. Brand), rat anti-L'sc (1:100) (a gift from S. Crews), Guinea pig anti-Tll (1:100) and Rabbit anti-Tll (1:500, gifts from J. Jäger) (Kosman et al., 1998), Guinea pig anti-PatJ, (1:500) (a gift from M. Krahn) (Sen et al., 2012), Rabbit anti-Cas3 (1:75, Cell Signaling), Rabbit anti-GFP (1:2000, Molecular Probes), Rabbit anti-βGal (1:1000, Cappel), Chicken anti-βGal (1:2000, Abcam). The following secondary antibodies were used: Alexa405, Alexa488, Alexa568 and Alexa647 (1:200, Molecular Probes). Phalloidin565 was used together with the secondary antibodies (1:1000, Molecular Probes).

Confocal stacks were acquired using a 63 × glycerol immersion objective on a Leica SP5 or a 40 × oil immersion objective on a Leica SPEII confocal microscope. Images were processed using ImageJ/FIJI and Adobe Photoshop. Figures and Illustrations were assembled in Adobe Illustrator.

2.4. Volume quantification

3D volumes of brains, proliferation centers, medulla cortex and lamina were quantified on confocal stacks (slice thickness $z = 1.5$ µm) with the TrackEM plugin of ImageJ/FIJI. On each 2D section entire brain lobes, neuroepithelia, medulla cortex and lamina were outlined. OPC and IPC neuroepithelia were identified by morphology by anti-Dlg staining and by absence of anti-Dpn staining, which marks neuroblasts. Medulla and lamina were identified by morphology and 3D volumes were reconstructed and quantified according to voxel size data. Five brains for control and experimental genotype were measured. Mean and standard deviation were calculated in Microsoft Excel. Significance was calculated with a Student's *t*-test and the *p*-values were assigned as $p < 0.05^{*}, < 0.01^{**}, < 0.001^{***}$.

3. Results

3.1. tll is dynamically expressed during larval optic lobe development

tll starts to be expressed in the developing optic placode at embryonic stage 11 and remains to be expressed in the optic lobe throughout embryogenesis (Green et al., 1993; Rudolph et al., 1997; Younossi-Hartenstein et al., 1997). After larval hatching *tll* expression is observed in the growing OPC and IPC (Fig. 1). Immunofluorescence labeling against endogenous Tll protein (Kosman et al., 1998) and a *tll::GFP* protein fusion construct (Venken et al., 2009) reveal uniform high expression in neuroepithelial cells of the OPC and IPC at 24 h and 48 h ALH (After Larval Hatching) (Fig. 1C, D, G, H, K). At 72 h ALH high *tll* and *tll::GFP* expression become restricted to neuroepithelial cells in the lamina furrow and lateral to the lamina furrow (LF), while more medial neuroepithelial cells downregulate *tll* expression (Fig. 1E, I, L, M). At 96 h ALH *tll* and *tll::GFP* expression remain high within and lateral to the lamina furrow (Fig. 1F, J). At 72 h and 96 h ALH additional Tll positive cells are observed in the medulla cortex, which

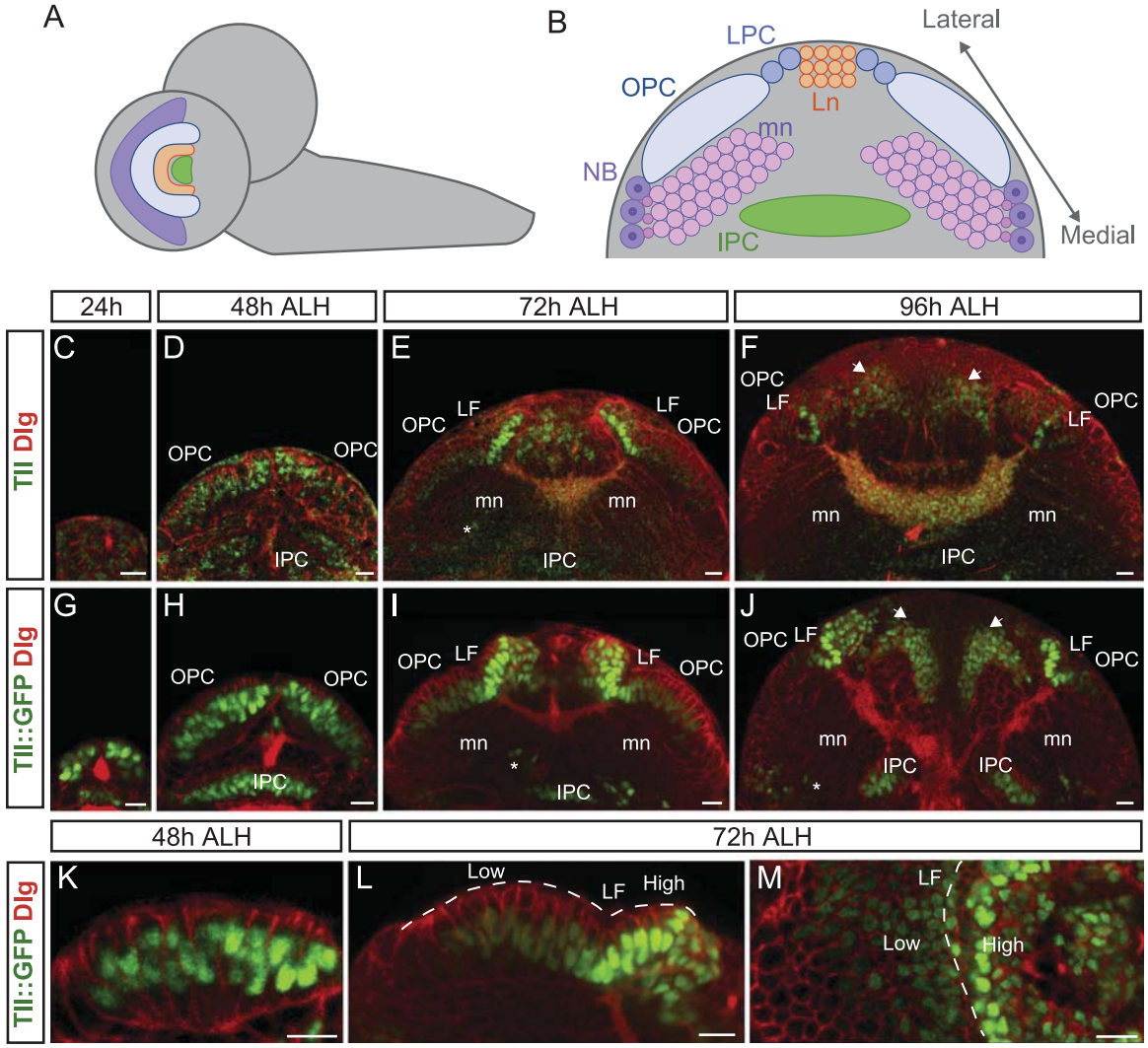

Fig. 1. Dynamic *tll* expression pattern in the optic lobe during larval development. (A, B) Illustrations of the larval brain and optic lobe, (A) shows lateral view and (B) shows frontal section. (C–F) are anti-Tll antibody stainings and (G–M) are anti-GFP antibody stainings of Tll::GFP at 24 h, 48 h, 72 h and 96 h after larval hatching (ALH). Cell cortices and septate junctions are outlined by anti-Dlg. All images show single frontal sections, except (M) shows a lateral section. At 24 h and 48 h ALH *tll* and *tll::GFP* are strongly expressed in neuroepithelial cells of the developing OPC and IPC (C, D, G, H and higher magnification K). At 72 h and 96 h a low and a high *tll* and *tll::GFP* expression domain becomes apparent in the developing OPC neuroepithelium (E, F, I, J and higher magnification L, M). *tll* and *tll::GFP* are also visible in most medial medulla neuroblasts (E, I, J, asterisk) and in progenitor cells and neurons deriving from the IPC (F, J, arrowheads). OPC: outer proliferation center, IPC: inner proliferation center, LF: lamina furrow. Scale bars: 10 µm.

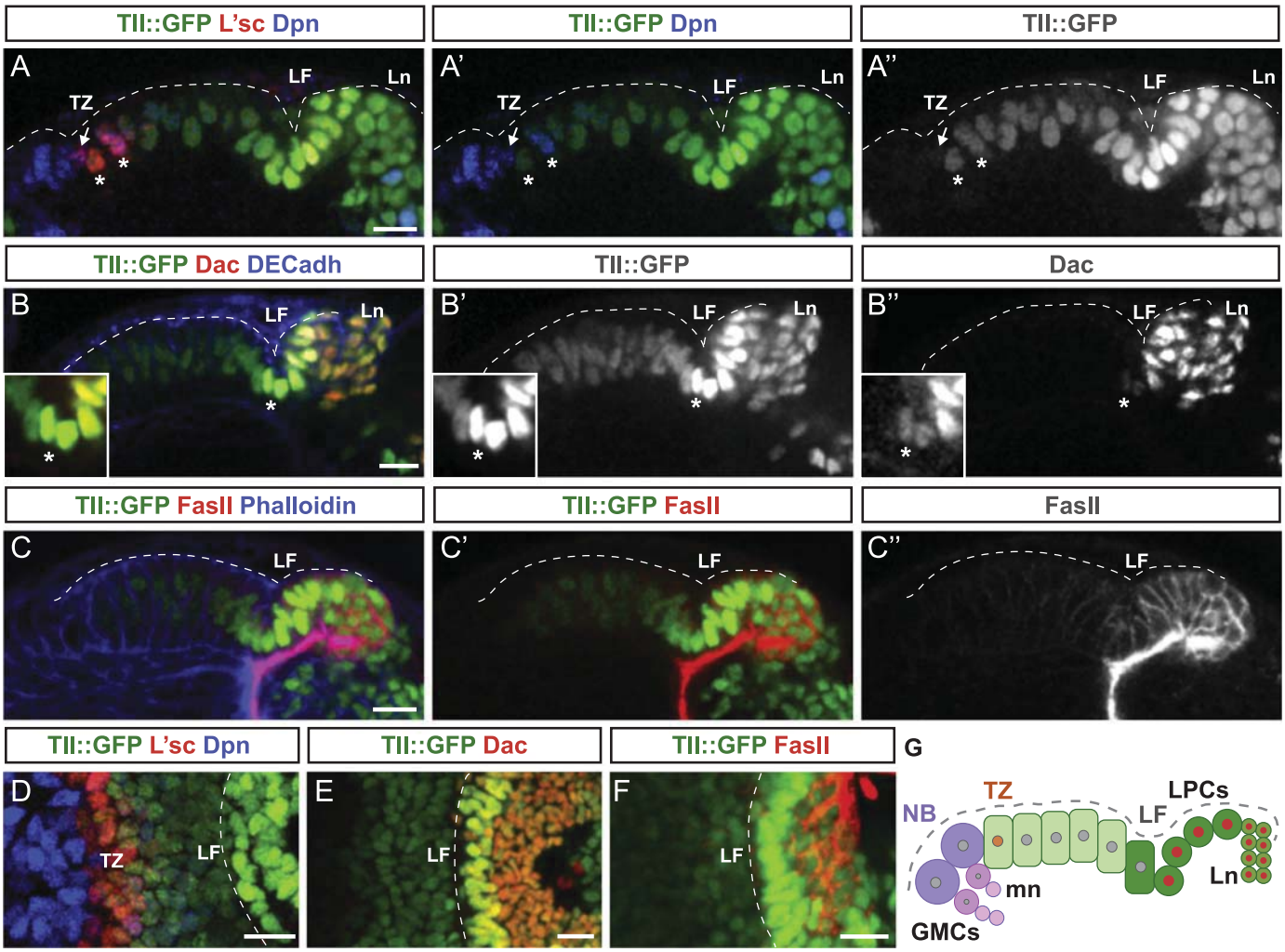

Fig. 2. Tll reveals a low- and a high-expression domain in the developing OPC. (A–C) are single frontal sections and (D–F) are lateral maximum projections of the OPC neuroepithelium at 72 h ALH. (A–A'' and D) the low *tll::GFP* expression domain starts at the neuroepithelial cell to neuroblast transition zone (TZ) marked by the expression of L'sc (asterisks) and extends to the lamina furrow (LF). A high *tll::GFP* expression domain includes the lamina furrow and lamina precursor cells. Presumptive lamina neurons show intermediate levels of *tll:GFP* expression. (B–B'' and E) the onset of high *tll::GFP* expression (asterisk) coincides with the LPC marker Dac. Co-expression of intermediate levels of *tll::GFP* and Dac is maintained in differentiating lamina neurons (Ln). (C–C'' and F) Fas II is a second marker that is co-expressed in LPCs with high *tll::GFP*. Cells are outlined by anti-DECad (B) or Phalloidin (C). (G) shows a schematic representation of *tll::GFP* (green), L'sc (orange) and Dac (red) expression. NB: neuroblasts, TZ: transition zone, LF: lamina furrow, NE: neuroepithelium, LPCs: lamina precursor cells, Ln: lamina neurons, GMCs: ganglion mother cells, Mn: medulla neurons. Scale bars: 10 μm.

correspond to the earliest born medulla neuroblasts at the very medial edge of the OPC (Fig. 1E, I, J, asterisk) (Li et al., 2013). At 96 h ALH another group of Tll positive cells is visible deeper in the optic lobe below the OPC epithelia. This group of progenitor cells has recently been described to be deriving from the IPC (Fig. 1F, J, arrowheads) (Apitz and Salecker, 2015). In the following we describe *tll* expression in more detail in the developing OPC.

3.2. *tll shows a low- and a high-expression domain in the developing OPC*

Since endogenous *tll* expression is accurately mirrored by *tll::GFP* expression we decided to analyze the expression pattern of *tll* in more detail using this construct. At 72 h ALH two *tll::GFP* expression domains can be distinguished in the developing OPC (Fig. 2). A low-expression domain starts at the neuroepithelial cell to medulla neuroblast transition zone and extends to the lamina furrow. *tll::GFP* expression is present in the low *deadpan (dpn)* expressing progenitors (also referred as PI progenitors cells) and is also expressed at low levels in Lethal of scute (L'sc) positive cells, which correspond to the transition zone (Fig. 2A asteriks, and D) (Yasugi et al., 2008, 2010). *tll::GFP* expression is downregulated in the most medial L'sc positive cell (Fig. 2A, arrow) and not detectable in adjacent Dpn positive medulla neuroblasts (Fig. 2A). At the lamina side of the OPC *tll::GFP* is expressed at high levels in cells within and lateral from the lamina furrow. *tll::GFP* expression is then downregulated and at intermediate levels in lamina neurons (Ln) (Fig. 2A).

The transcription factor Dachshund (Dac) is an early marker for lamina precursor cells (LPCs) and is required for lamina neuronal differentiation (Mardon et al., 1994; Huang and Kunes, 1996; Chotard et al., 2005). We found that high *tll::GFP* expression starts in the lamina furrow in the first cell that stains positive for Dac expression (Fig. 2B, asterisk and E). High *tll::GFP* expression is maintained in all Dac positive LPCs and at intermediate levels in lamina neurons (Fig. 2B, E). A second marker that we found to be co-expressed with *tll::GFP* in LPCs and in new born lamina neurons is Fasciclin II (FasII), the *Drosophila* homolog of mammalian NCAM (Pereanu et al., 2005). Interestingly, similarly to *tll::GFP* expression Fas II reveals a lateral high and a medial low expression domain in the developing OPC (Fig. 2C and F).

Hence, *tll* is differentially expressed in specific domains of the developing OPC: low-expression is detected in the medial OPC that includes the neuroepithelial cell to neuroblast transition zone and

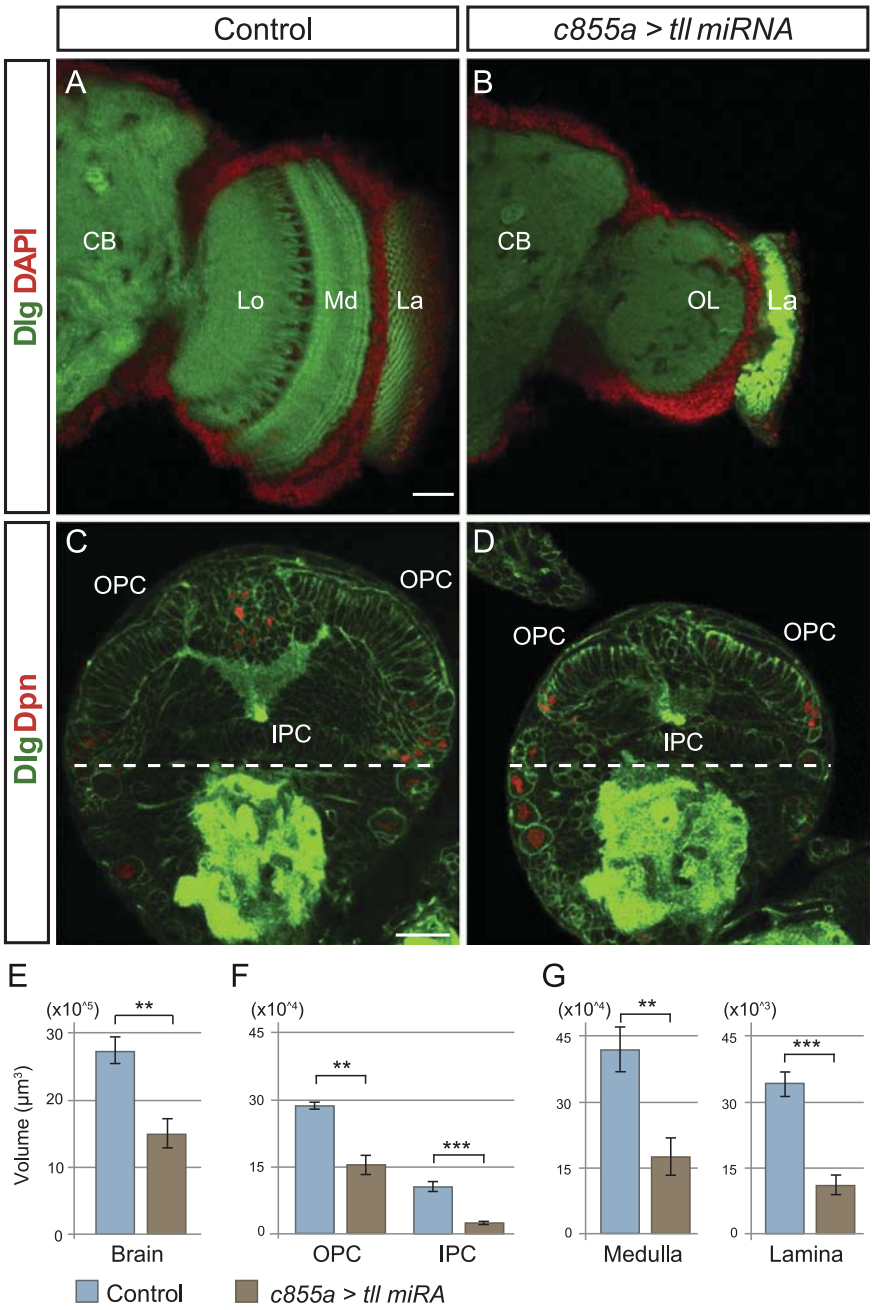

Fig. 3. *tll* knockdown affects development of optic ganglia. (A, B) are confocal sections of brain lobes at pharate pupal stage (C, D) are frontal sections of brain lobes at 72 h ALH stained for Dpn and Dlg and (E, F, G) show quantification by using 3D reconstructions of brains, proliferation centers, medulla cortex and lamina volumes. (A, B) in control brains (A) the optic ganglia lamina, medulla and lobula form clearly structured compartments in the optic lobe. In contrast, upon *c855a > tll*^{miRNA} expression (B) all optic lobe ganglia are severely reduced. While the lamina ganglion is still visible, medulla and lobula ganglia are not distinguishable as individual compartments any more. There are no morphological changes visible in the central brain. (C, D) The *tll* knockdown phenotype is already apparent in the developing larval optic lobe. In *c855a > tll*^{miRNA} the entire optic lobe (D) is significantly smaller than the control optic lobe (C) while the central brain seems to be unaffected; quantification in (E). OPC and IPC are significantly reduced; quantification in (F). Dashed lines indicate the border between optic lobe and central brain. Lamina and medulla cortex are significantly reduced in *c855a > tll*^{miRNA} optic lobes when compared to control brains; quantified in (G). Error bars represent the Standard Error of the Mean, SEM; p-value $< 0.05^{*}$, p-value $< 0.01^{**}$ and p-value $< 0.001^{***}$. CB: central brain, OL: optic lobe, Lo: Lobula, Md: Medulla, La: Lamina, OPC: Outer proliferation center, IPC: Inner proliferation center. Scale bars: 25 µm.

extends to neuroepithelial cells medially adjacent to the lamina furrow; high-expression is detected in neuroepithelial cells in the lamina furrow, in which Dac and FasII positive LPCs are located. Finally, we found *tll::GFP* expression at intermediate levels in lamina neurons.

3.3. *tll knockdown affects neurogenesis and leads to disrupted optic ganglia*

In order to study the functional role of *tll* in optic lobe development we used a previously established microRNA construct to knockdown *tll* expression (*tll*^{miRNA}) (Lin et al., 2009; see Fig. S2). The expression of a *UAS-tll*^{miRNA} construct was driven in the OPC and IPC from first larval instar onwards with the GAL4 driver line *c855a* (*c855a > tll*^{miRNA}) (Manseau et al., 1997; Egger et al., 2007). Since only a small number of adults eclosed, we examined the optic lobe in pharate pupae (Fig. 3). In control brains the lamina, medulla, lobula and lobula plate form structurally distinct optic ganglia. In *c855a > tll*^{miRNA} animals the entire optic lobe is significantly reduced in size. In addition, with the exception

of the lamina, the other optic ganglia cannot be distinguished from each other ($n=5$ brains) (Fig. 3A, B).

In order to analyze optic lobe development during earlier stages we stained larval brains at 72 h ALH with antibodies against the cell outline marker Discs large (Dlg) and the neuroblast marker Dpn. Strikingly, the *c855a > tll*^{miRNA} larval brains are 1.7 times smaller as compared to control brains (Fig. 3C, D). Quantification reveals a mean volume of 27×10^5 μm^3 for control brains versus a mean volume of 16×10^5 μm^3 for *c855a > tll*^{miRNA} brains (SD= 4.3×10^5 μm^3, $n=5$ for control; SD=4.9×10^5 μm^3, $n=5$ for *c855a > tll*^{miRNA}) (Fig. 3E).

Measurement of optic lobe proliferation centers OPC and IPC reveals a drastic reduction in size upon *tll* knockdown. The size of the OPC is reduced by a factor of 1.8 (Mean Vol=16×10^4 μm^3, SD=4.8×10^4 μm^3, $n=5$), while the size of the IPC is reduced by a factor of 3.6 (Mean Vol=3×10^4 μm^3, SD=0.7×10^4 μm^3, $n=5$) as compared to control brains (OPC Mean Vol=29×10^4 μm^3, SD=1.6×10^4 μm^3, $n=5$; IPC Mean Vol=11×10^4 μm^3, SD=2.4×10^4 μm^3, $n=5$) (Fig. 3F). Furthermore, quantification reveals that the medulla cortex and the lamina are severely reduced in size upon *tll* knockdown. The size of the medulla is reduced by a factor of 2.4 (Mean Vol=17×10^4 μm^3, SD=9.4×10^4 μm^3, $n=5$) while the size of the lamina is reduced by a factor of 3.1 (Mean Vol=11×10^3 μm^3, SD=2×10^3 μm^3, $n=5$) as compared to control brains (Medulla Mean Vol=41×10^4 μm^3, SD=11×10^4 μm^3, $n=3$; Lamina Mean Vol=34×10^3 μm^3, SD=6×10^3 μm^3, $n=5$) (Fig. 3G).

The severe reduction in size observed in the developing proliferation centers and ganglia of *c855a > tll*^{miRNA} optic lobes suggest that *tll* has an important role in the specification of optic lobe neural precursor cells. Apitz and Salecker have recently shown that *tll* is involved in a transition between two more mature progenitor cell states in the developing IPC. They have further demonstrated that *RNAi* against *tll* from early larval stages onwards leads to a complete loss of IPC structures (Apitz and Salecker, 2015). Our observations are in agreement with these findings and support a role for *tll* at early larval stages in the proliferating IPC.

The failures in growth and compartmentalization of defined optic ganglia in *c855a > tll*^{miRNA} might be due to misspecification of optic lobe stem or progenitor cells or to impaired production of neurons. In the following we focus on the developing OPC, which harbors the progenitor cells for the medulla and the lamina and

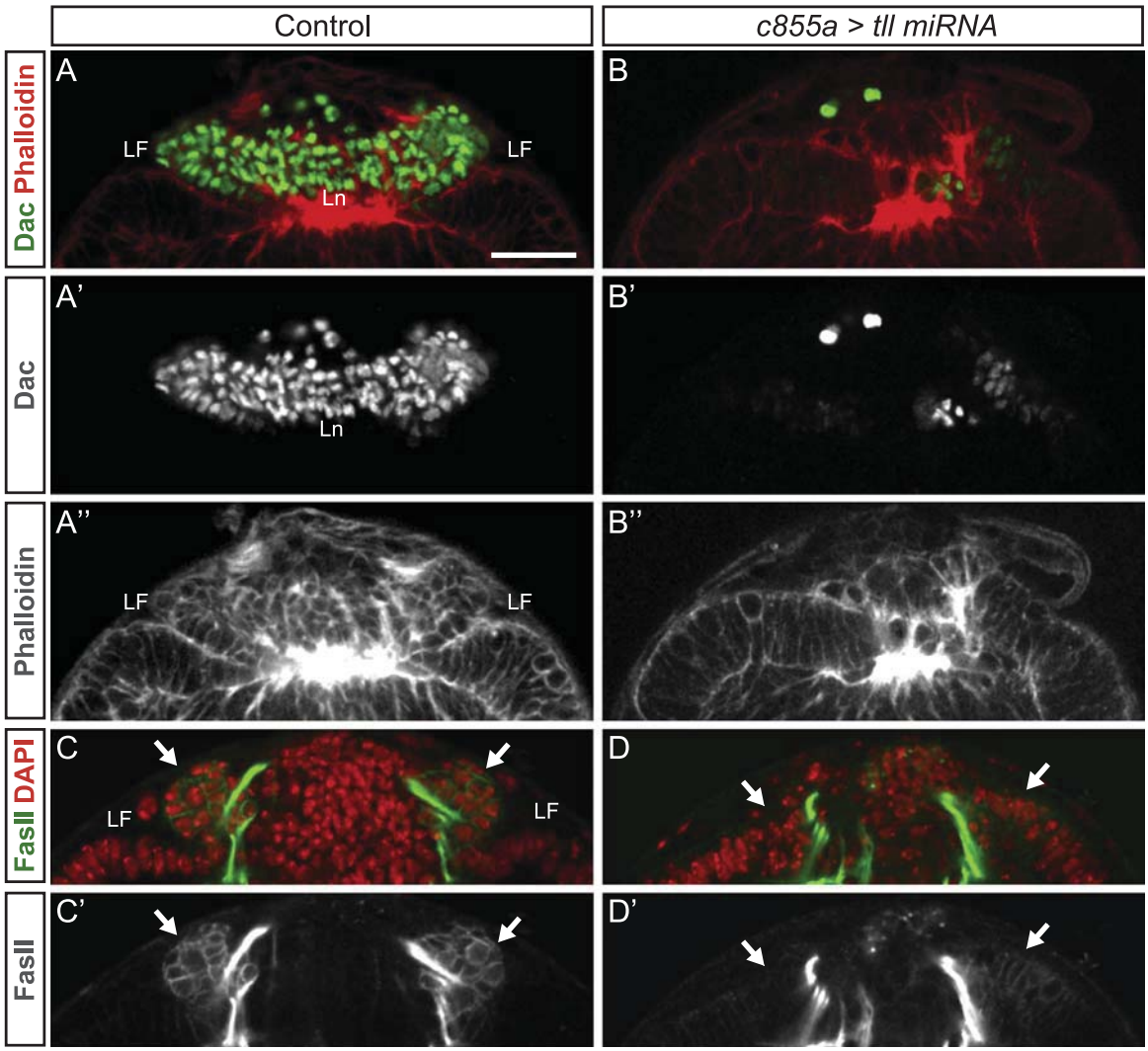

Fig. 4. *tll* knockdown leads to a reduction in Dac positive lamina neurons and changes in neuroepithelium morphology. (A–D) are single frontal sections at 72 h ALH. (A–A'', B–B'') in control brains Dac positive neurons form well-structured columns in the developing lamina (A, A'). In contrast, upon *c855a > tll*^{miRNA} knockdown Dac positive lamina neuronal columns are largely absent or disorganized (B, B'). In control brains (A'') at 72 h ALH a deep groove is visible in the lateral OPC neuroepithelium that corresponds to the lamina furrow (LF). In *c855a > tll*^{miRNA} knockdown brains (B'') the morphology of the lateral OPC neuroepithelium is changed and the lamina furrow is not apparent. In control brains, Fas II is strongly expressed in LPCs (C, C', arrows) and significantly reduced in presumptive LPCs upon *c855a > tll*^{miRNA} knockdown (D, D', arrows). Phalloidin stains cell outline. Ln: Lamina neurons, LF: Lamina furrow, LPCs: Lamina precursor cells. Scale bar: 25 μm.

where *tll* function has so far not been characterized.

3.4. *tll is required for lamina precursor cell specification*

In the developing OPC *tll* expression is detectable at high and intermediate levels in LPCs and differentiating lamina neurons, respectively. We therefore addressed the question whether *tll* is required for the specification of LPCs and subsequently for lamina neurogenesis. The transcription factor Dac is a marker for LPCs and differentiating lamina neurons, the latter are arranged in characteristic columns in the developing lamina (Fig. 4A) (reviewed in Ting and Lee, 2007). When *tll* expression is knocked down in *c855a > tll^{miRNA}* animals from early larval stages onwards, lamina columns are severely disrupted and the number of Dac positive cells is greatly reduced (Fig. 4B). Interestingly, impaired *tll* function leads also to morphological changes in the OPC neuroepithelia. At 72 h ALH a deep grove, the lamina furrow is visible in the lateral OPC (Fig. 4A) whereas in *c855a > tll^{miRNA}* animals the lamina furrow is reduced or completely absent at this stage (Fig. 4B).

In order to assess whether the specification of LPCs is affected by impairing *tll* function we analyzed the cell adhesion molecule Fas II that strongly marks the cell membranes of LPCs laterally to the lamina furrow and of newly born lamina neurons (Fig. 4C arrow). Interestingly, in *c855a > tll^{miRNA}* knockdown brains, Fas II expression was lost or significantly reduced in LPCs and lamina neurons, indicating a failure in LPCs specification and the generation of lamina neurons (Fig. 4D, arrow).

Since in *c855a > tll^{miRNA}* brains *tll* expression is impaired in the entire optic lobe and not only in LPCs we tested the cell-autonomous requirement of *tll* expression by clonal *tll^{miRNA}* knockdown and *tll^{l49}* loss-of-function experiments. Clones were induced at 24 h ALH by using the Flip-out or the MARCM technique and optic lobes were analyzed at 72 h ALH. It is evident that clonal knockdown of *tll* expression in the LPCs domain leads to drastic reduction of Dac expression (Fig. 5A, B, white arrowhead) as compared to non-clonal control LPCs in the same brain (Fig. 5A, B, yellow arrowhead) ($n=7$ clones). Clonal knockdown of *tll* in domains of differentiating lamina neurons exhibits a loss of Dac staining (Fig. 5A, arrow) ($n=5$ clones). Similarly, a loss of Dac expression was also observed in *tll^{l49}* loss-of-function clones (Fig. S3A, B) ($n=5$ clones). Apitz and Salecker described that RNAi against *tll* in the entire IPC leads to reduced Dac positive lobula plate neurons (Apitz and Salecker, 2015). We have made similar observations and our clonal knockdown experiments demonstrate that *tll* regulates Dac expression in a cell-autonomous manner in lobula plate neurons (Fig. 5B, arrow) ($n=6$ clones).

In order to address whether *tll* is cell-autonomously required for Fas II expression in LPCs we induced knockdown clones in a similar manner as described above. LPCs with impaired *tll* expression revealed a clear reduction of Fas II staining (Fig. 5C, white arrowhead) as compared to non-clonal LPCs (Fig. 5C, yellow arrowhead) ($n=4$ clones).

In order to test whether *tll* is sufficient to convert unspecified neuroepithelial cells towards a lamina fate we used either the *c855a-Gal4* driver line or the Flip-out clonal system to misexpress *tll* in neuroepithelial cells. While *c855a > tll* animals die at second larval instar, clonal *tll* misexpressing cells within the neuroepithelium do not show any characteristics of LPCs i.e. they do not

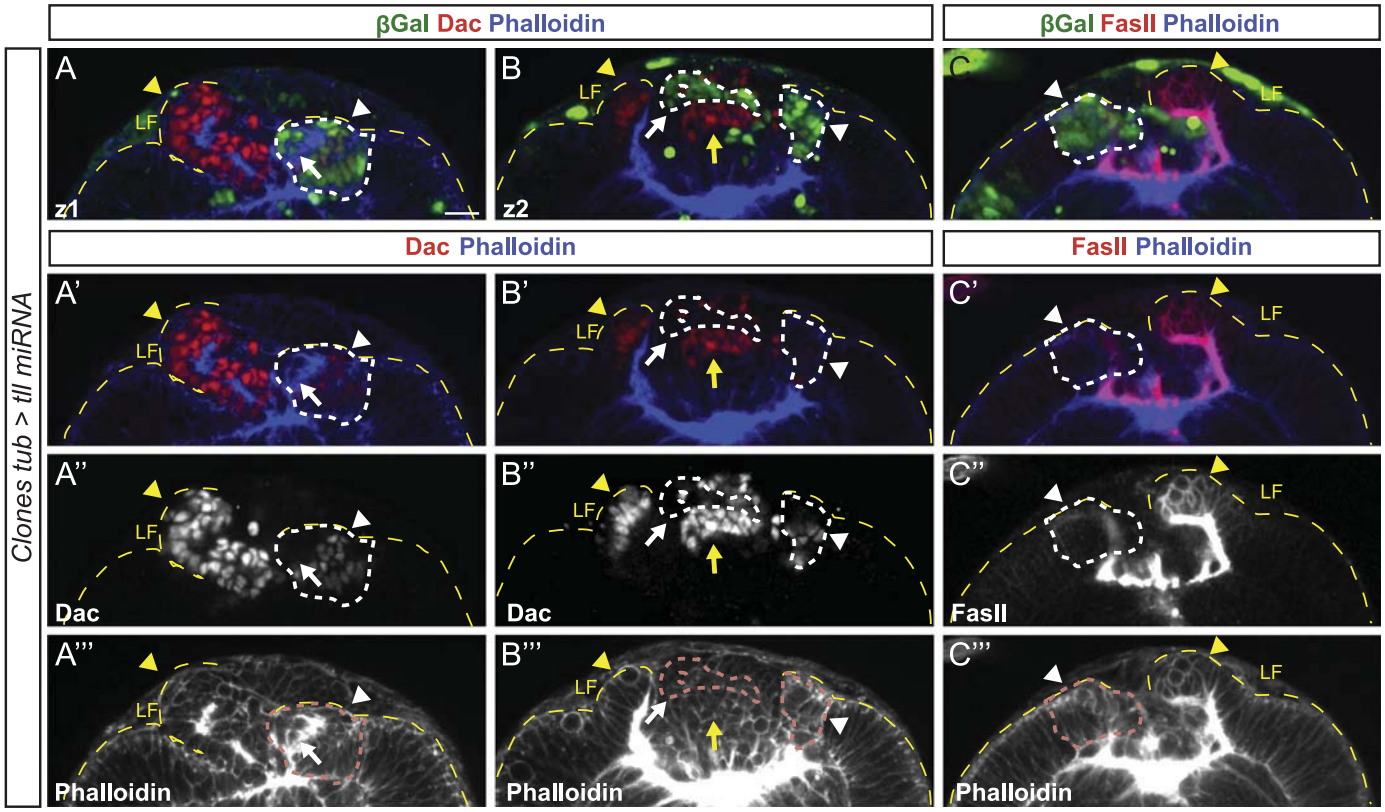

Fig. 5. *tll* regulates LPC specification and lamina neurogenesis in cell-autonomous manner (A–C) single frontal sections at 72 h ALH. βGal staining labels *tll* knockdown clones. (A, B) two sections in the same brain in ventral z1 and more dorsal z2 position. (A–A‴, B–B‴) LPCs and lamina neurons reveal high Dac expression (A–A″ and B–B″, yellow arrowheads) as well as lobula plate neurons deriving from the IPC (B–B″, yellow arrow). Upon clonal *tll* knockdown, Dac expression in LPCs (A–A″ and B–B″, white arrowheads), lamina neurons (A–A″, white arrows) and lobula plate neurons (B–B″, white arrows) is significantly reduced or absent. (C–C‴) LPCs express the cell adhesion molecule Fas II (C–C″, yellow arrowheads). Upon clonal *tll* knockdown Fas II expression is significantly reduced in LPCs (C–C″, white arrowheads). (A‴, B‴, C‴) Clonal knockdown of *tll* results in morphological changes within the neuroepithelium. While on the non-clonal control side (yellow arrowheads) a groove in the neuroepithelium, the lamina furrow (LF), is clearly visible, on the clonal side (yellow arrowheads) the lamina furrow is diminished. Phalloidin stains cell outline. Scale bar: 10 μm.

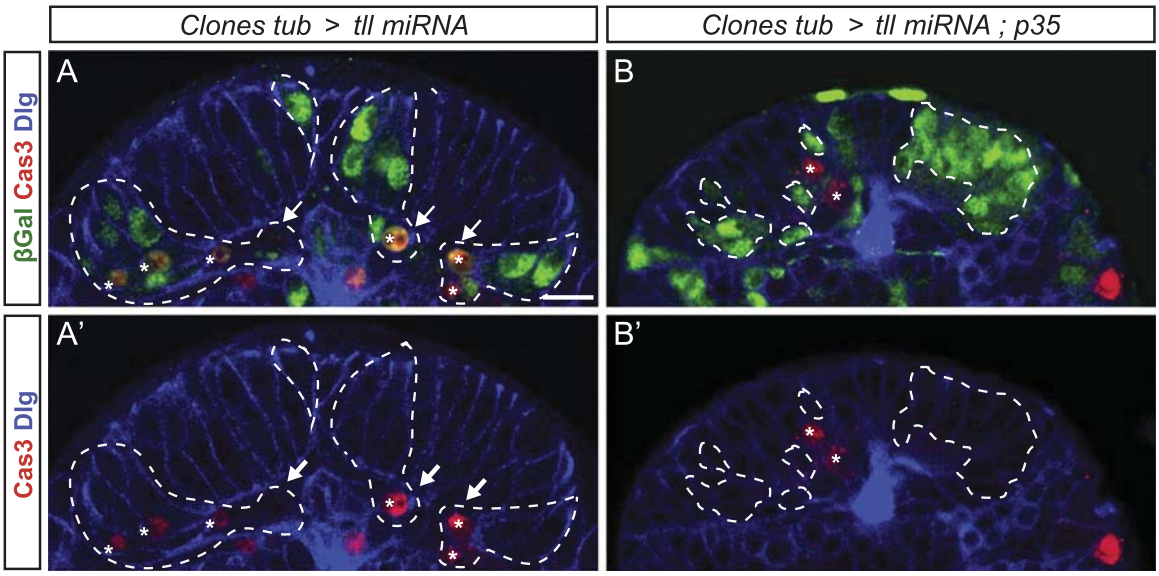

Fig. 6. *tll* is required for neuroepithelial cell survival. (A and B) show single frontal sections at 48 h ALH. (A–A') *tll* knockdown clones show an increased number of cells that stain for the apoptotic marker cleaved Caspase 3 (Cas3, asterisk). A few cells show Cas3 staining within the neuroepithelium while many Cas3 positive cells are extruded from the neuroepithelium (white arrows) and become aberrantly localized in the medulla cortex. (B–B') *tll* knockdown clones simultaneously expressing anti-apoptotic *p35* are no longer enriched with Cas3 positive cells (asterisk) and remain within the neuroepithelium. Scale bar: 10 μm.

ectopically express the LPC marker Dac (Fig. S4A) ($n=4$ clones).

Together, these results suggest that Tll is required in a cell-autonomous manner to specify characteristics of LPCs during specification and maturation and is necessary for the proper generation of lamina neurons. However, elevated *tll* expression appears not to be sufficient to induce the LPC fate in more medial undifferentiated neuroepithelial cells.

3.5. *tll is required for neuroepithelial cell survival*

tll Is expressed at high levels throughout the OPC neuroepithelium during early larval stages (Fig. 1) and neuroepithelial knockdown leads to a markedly reduced optic lobe ganglia (Fig. 3E, F, G). Hence we assessed whether *tll* has an early function in neuroepithelial cells during phases of optic lobe neuroepithelial proliferation and growth. We induced knockdown clones at 12 h ALH and examined brains at 48 h ALH (Fig. 6). We noticed that clonal cells with impaired *tll* function are extruded from the neuroepithelium and become aberrantly localized in the medulla cortex (Fig. 6A, arrows). A similar phenotype has been recently reported for clones that are mutant for the transcription factor Optix. Neuroepithelial cells lacking Optix function are extruded from the neuroepithelium and undergo apoptosis (Gold and Brand, 2014). Hence we assessed, whether *tll* is similarly required for cell survival and stained clones for the cell apoptosis marker cleaved Caspase-3 (Cas3). Indeed, clonal cells with impaired *tll* function show increased Cas3 expression in the neuroepithelium (Fig. 6A, asterisks) and in the medulla cortex (Fig. 6A, arrows). Larval brains, in which we induced wildtype clones contained in average 12 Cas3 positive cells in the OPC (SD=6.7, $n=5$ brain lobes), while only 32% of these Cas3 positive cells where clonal cells ($Cas3^+$, βGal^+ cells). In contrast, larval brains, in which we induced *tll* knockdown clones, contained in average 31 Cas3 positive cells in the OPC whereas 77% of those were clonal cells (SD=10.8, $n=6$ brain lobes).

We wondered whether basal extrusion of neuroepithelial cells is a consequence of cell death or whether cells undergo cell death because they loose epithelial integrity upon *tll* knockdown. Therefore, we aimed to prevent apoptosis in *tll* knockdown clones by inducing the baculovirus anti-apoptotic gene *p35*, which encodes a broadly acting caspase inhibitor (Hay et al., 1994; Clem, 2001). Indeed, in *tll* knockdown clones that simultaneously express *p35* the apoptosis marker Cas3 is absent. Furthermore, blocking apoptosis leads to large clones that remain within the neuroepithelium (Fig. 6B) ($n=8$ brain lobes). However, these clonal cells are not arranged in well-organized columnar epithelia but show signs of disintegration when compared to the neighboring wiltype epithelial cells. This phenotype differs from *optix* loss-of-function clones, in which apoptosis is inhibited. *optix* mutant clones with induced *p35* are sorted out from the wildtype neuroepithelium and form ectopic neuroepithelial rosettes in the underlying medulla cortex (Gold and Brand, 2014).

Our data suggests that *tll* function is required in the proliferating neuroepithelium for cell survival. Epithelial integrity, which is lost upon *tll* knockdown can only partially be restored by blocking apoptosis. Hence we favor the idea that initiation of the cell death program may be triggered by impaired neuroepithelial integrity and that apoptotic cells are subsequently cleared away from the neuroepithelium through basal extrusion.

3.6. *Impaired tll function affects the neuroepithelial morphology and the neuroepithelial cell to neuroblast transition zone*

Blocking of apoptosis through induced *p35* led to larger clones that stayed within the neuroepithelium and frequently included the neuroepithelial cell to neuroblast transition zone. In analyzing these clones with neuroepithelial and transition zone markers we found two additional striking phenotypes. Firstly, large tll^{miRNA}, *p35* clones revealed abnormal epithelial morphology, which included ectopic folds (Fig. 7A, open arrow) and furrows (Fig. 7A, white arrow) ($n=6$ brain lobes). Interestingly, furrows were mostly visible at the border between clonal and wildtype cells (Fig. 7A, white arrow). We further examined neuroepithelial cells with two epithelial marker proteins. PatJ is a member of the Cumbs/Stardust complex, which localises at subapical region in epithelial cells. Dlg forms a complex with Scribbles (Scrib) and Lethal giant larvae (Lgl) at basolateral septate junctions (reviewed in Bilder, 2004; Tepass, 2012). Interestingly, while we do not find any change in levels for PatJ in *tll* knockdown clones, we observed an increased signal for Dlg protein at the basolateral side of clonal

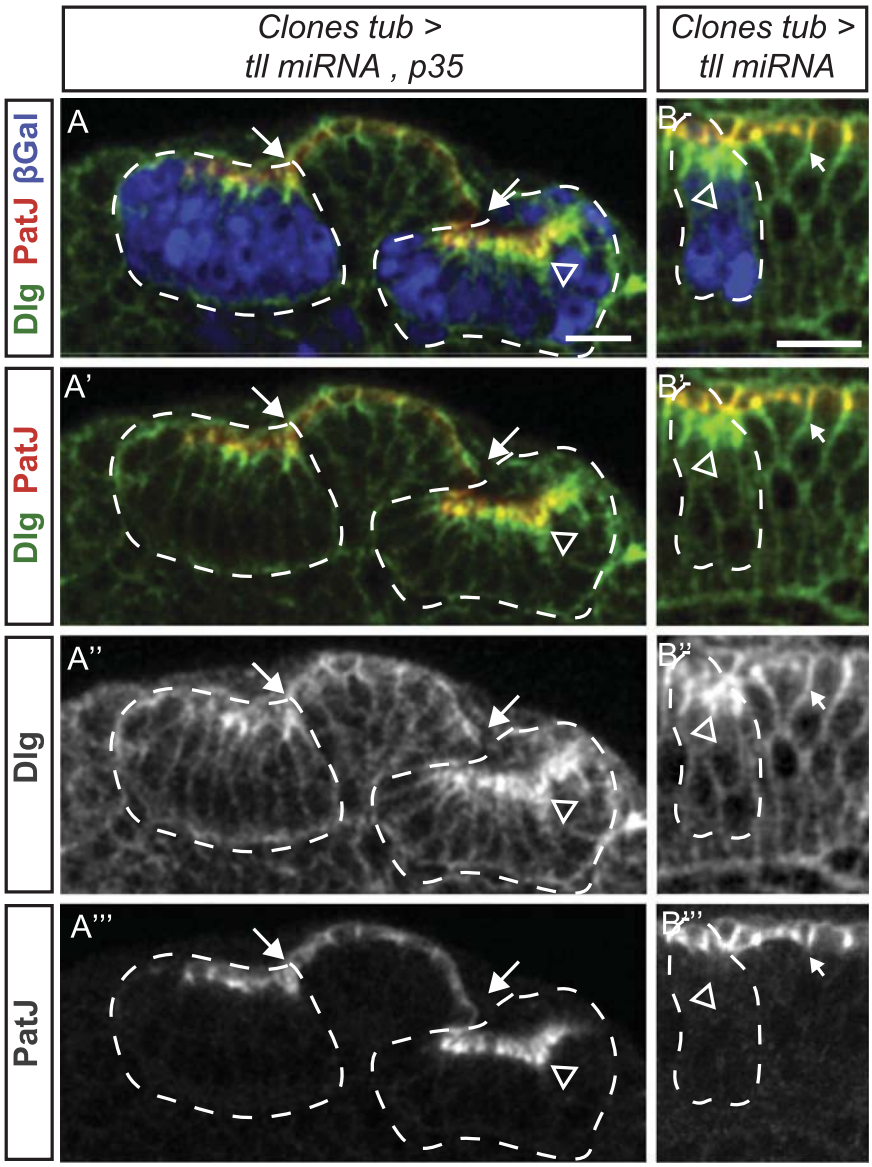

Fig. 7. Neuroepithelial cells properties are impaired upon *tll* knockdown. (A and B) show single frontal sections at 72 h ALH. (A–A‴) expression of anti-apoptotic *p35* in *tll* knockdown clones results in large clones that remain within the neuroepithelium. Epithelial constrictions and ectopic folds are visible at the interface between clonal and wildtype cells (white arrows). (B–B‴) a *tll* knockdown clone shows enriched signal for the basolateral protein Dlg (open arrows) while no gross abnormalities are visible for the subapical marker PatJ as compared to neighboring wildtpye cells (white arrow). Scale bars: 10 μm.

cells (Fig. 7B, open arrow) as compared to neighboring wildtype cells (Fig. 7B, arrow) ($n=10$ brain lobes).

Secondly, we examined whether impaired *tll* function affects the neuroepithelial cell to neuroblast transition zone. In the OPC neuroepithelium a proneural wave of L'sc expression coincides with the transition from neuroepithelial cells to Dpn positive neuroblasts (Yasugi et al., 2008). We observed that large tll^{miRNA}, *p35* clones that span the transition zone include neuroepithelial cells and Dpn positive neuroblasts (Fig. 8A). Hence, *tll* knockdown does not seem to affect the transformation of neuroepithelial cells into neuroblasts. However, careful examination of the clones revealed a very mild delay of one cell row in the upregulation of Dpn (Fig. 8A, arrows) ($n=4$ clones). A similar phenotype has been reported in mutant clones, which are deficient for the three genes *ac*, *sc* and *l'sc* genes of the *acheate-scute* complex (Yasugi et al., 2008). Therefore, we looked at *l'sc* expression in tll^{miRNA} knockdown or tll^{l49} mutant MARCM clones. To our surprise, clonal knockdown or loss-of-function of *tll* resulted in a complete lack of L'sc expression in the neuroepithelial cell to neuroblast transition zone (Fig. 8B, Fig. S3C) ($n=6$ clones, $n=4$ clones). We wondered whether *tll* is sufficient to induce *l'sc* expression in neuroepithelial cells. However, this is not the case since clonal *tll* misexpression did not lead to upregulation of L'sc expression in more lateral neuroepithelial cells (Fig. S4B) ($n=4$ clones).

We conclude that Tll regulates the levels of Dlg protein at the basolateral side of neuroepithelial cells and controls neuroepithelial cell morphology. Furthermore, Tll is required for the expression of the proneural gene *l'sc* in the neuroepithelial cell to neuroblast transition zone but it is not sufficient to induce *l'sc* and the transformation of neuroepithelial cells into neuroblasts.

4. Discussion

In the developing *Drosophila* optic lobe symmetric divisions of neuroepithelial cells initially leads to rapid growth. In subsequent phases at the medial edge of the OPC neuroepithelial cells transform into asymmetrically dividing medulla neuroblasts, while at

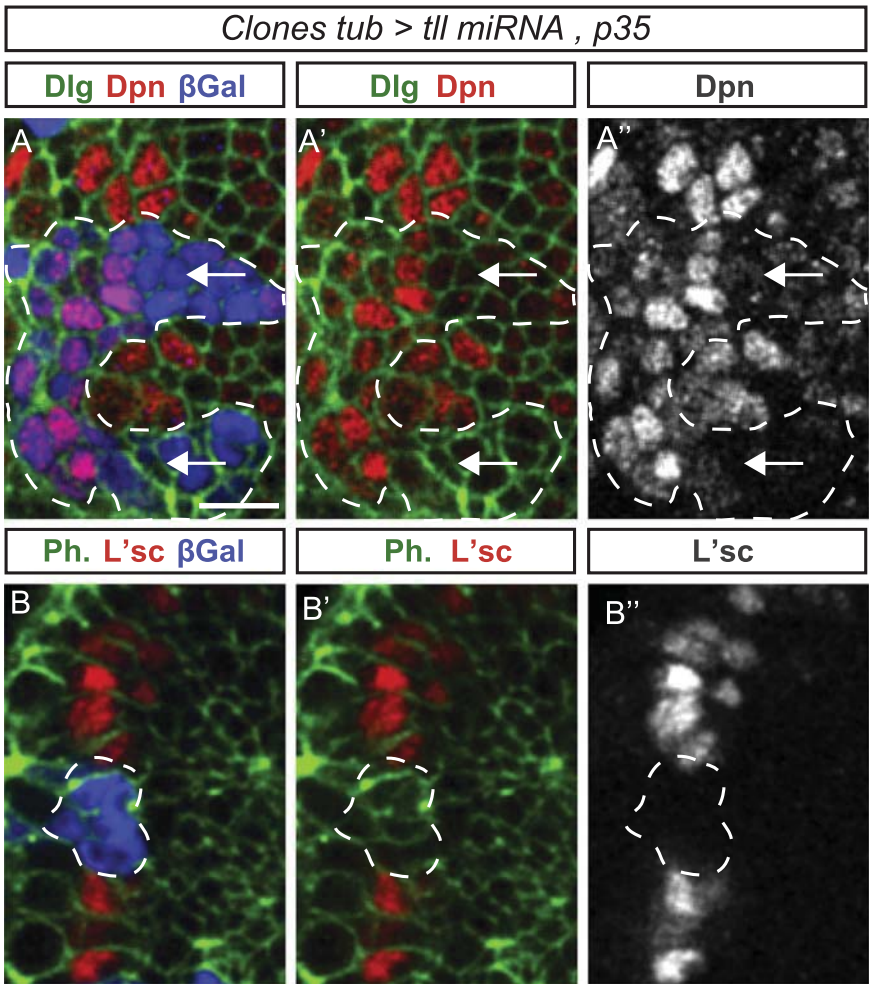

Fig. 8. *tll* is required for the timing of the neuroepithelial cell to neuroblast transition. (A and B) show single lateral sections at 72 h ALH. (A–A″) shows a *tll* knockdown clone expressing the anti-apoptotic *p35*, which spans over the neuroepithelial cell to neuroblast transition zone. Comparing clonal cells to neighboring wildtype cells reveals a delay of one cell row in the upregulation of neuroblast marker Dpn (A, arrows). (B–B″) shows a *tll* knockdown clone expressing the anti-apoptotic *p35*, which is located in the neuroepithelial cell to neuroblast transition zone. L'sc expression is completely absent in clonal cells. Dlg (A–A″) and Phalloidin (Ph., B–B″) stain cell outline. Scale bar: 10 μm.

the lateral side neuroepithelial cells become lamina precursor cells (reviewed in Apitz and Salecker, 2014). IPC precursor cells leave the neuroepithelium in migratory streams and form secondary proliferation zones that generate neurons of the lobula and lobula plate (Apitz and Salecker, 2015). We find that knockdown of *tll* in optic lobe neuroepithelia, from early larval stages onwards affects all optic ganglia in the adult brain. The lamina is severely reduced in size while medulla, lobula and lobula plate do not form morphologically distinct compartments as seen in normal brains. These results indicate that *tll* has multiple roles during optic lobe development that involve both the outer and the inner proliferating centers (OPC and IPC).

We found that *tll* is dynamically expressed in neuroepithelial cells of the developing OPC and IPC during proliferation and differentiation phases. Initially, *tll* is expressed uniformly at high levels throughout the OPC and IPC neuroepithelia. During this early period of optic lobe growth we found that *tll* is required for cell survival. Upon clonal *tll* knockdown cells within the OPC upregulate the apoptotic marker cleaved Cas3 and are extruded from the neuroepithelium. Upregulated apoptosis might be in part responsible for the growth defects that we observe in larval and pharate pupal optic lobes with impaired *tll* function. However, misregulated cell death might not be the sole reason for the severe reduction in optic ganglia size. Mutations in the gene coding for the Six3/6 transcription factor Optix have previously been described to have a similar apoptosis phenotype in the developing optic lobe (Gold and Brand, 2014). However, there are clear phenotypic differences between the *optix* and the *tll* mutant clones in which apoptosis is blocked. While *optix, p35* mutant clones are sorted away from the neuroepithelium (Gold and Brand, 2014), tll^{miRNA}, *p35* knockdown clones remain embedded within the neuroepithelium. Therefore, although mutations in both genes lead to abnormalities in epithelial morphology and cell apoptosis the two factors might act in different genetic pathways.

At a later stage during larval development we observed the appearance of two distinct expression domains in the proliferating OPC neuroepithelium. A low *tll* expression domain extends from the neuroepithelial cell to neuroblast transition zone to the lamina furrow whereas a high *tll* expression domain starts at the lamina furrow and includes the lamina precursor cells (LPCs). Intermediate levels of *tll* expression domain are seen in lamina neurons that derive from LPCs. Interestingly, the appearance of the two distinct expression domains in the OPC coincides with the formation of LPCs and the arrival of incoming axons from photoreceptor neurons. It has been shown that Hh signaling from incoming retinal axons triggers the release of LPCs from a G1 cell cycle arrest and initiates final differentiative symmetric divisions to generate pairs of lamina neurons (Huang and Kunes, 1996, 1998). Our data suggests that *tll* is involved in the early specification of LPCs since high *tll* expression is detectable prior to the

lamina furrow. Indeed, upon *tll* knockdown Dac, the earliest known marker is severely reduced in presumptive LPCs. A similar phenotype has been described for double loss-of-function mutants for glial cell missing genes (*gcm and gcm2*). The study demonstrates that Gcm together with the Hedgehog pathway is required to induce Dac in LPCs and to mediate lamina neurogenesis (Chotard et al., 2005). More recent work by Pineiro and colleagues shows that LPCs, similar to medulla progenitors cells, go through a sequence of different states that are characterized by the expression of transcription factors of the retinal determination network (RDN) (Pineiro et al., 2014). Although not in the scope of this work, future studies might reveal the relationship between Tll, Gcm and the RDN genes that control LPC specification and lamina neurogenesis. Our results suggest that impaired *tll* function leads to failures in the specification of lamina precursor cells, which might affect lamina neurogenesis.

We have currently no explanation other than increased apoptosis for what causes the reduced medulla cortex in the *tll* knockdown brains. However, to our surprise the proneural factor L'sc is completely absent in *tll* mutant clones spanning over the transition zone. Yasugi et al., has reported that a deficiency that removes three *acheate-scute* complex genes (sc^{19}), including *l'sc* leads to a mild delay in the neuroepithelial cell to neuroblast transition (Yasugi et al., 2008). Consistent with these results our clonal analysis indicates that the timing of the neuroepithelial cell to neuroblast cell fate transformation is weakly affected upon impaired *tll* function. We cannot exclude, however, that also other mechanisms, such as cell proliferation, are altered in the developing OPC neuroepithelia upon *tll* knockdown.

Interestingly, the *tll* homolog Tlx has crucial roles during embryonic and adult neurogenesis in the mammalian brain and retina (reviewed in Gui et al., 2011; Islam and Zhang, 2015). During embryonic cerebral cortex development when radial glial cell expand the pool of progenitor cells, Tlx prevents neural stem cells from prematurely adopting a more differentiated neural precursor state (Roy et al., 2004; Li et al., 2008). Of particular interest here is that Tlx is also expressed in progenitor cells in the developing retina and in the optic disk. In Tlx mutant mice initial specification seems normal but then cell numbers in each nuclear layer are progressively reduced at later stages (Miyawaki et al., 2004). Another study shows that retinas of Tlx loss-of-function mutant mice show a significant increase of apoptotic cells and a prolonged cell cycle of retinal progenitor cells (Zhang et al., 2006). Therefore, Tll and Tlx might have evolutionary conserved functions during visual system development. A few Tlx target genes have been identified, among them most prominently the tumor suppressor gene PTEN, which is repressed by Tlx in the mouse retina (Zhang et al., 2006). While it is currently unknown whether a similar interaction exist between Tll and Pten in the *Drosophila* optic lobe future studies will integrate Tll in genetic pathways that control neural progenitor cells.

Contributions

OG, SGS and BE designed the experiments. OG with help from BP and BE performed all experiments. OG, SGS and BE wrote the manuscript.

Acknowledgments

We thank A. Brand, J. Skeath, J. Jäger, J. Reinitz, B. Bello, H. Reichert, S. Crews and M. Krahn, the Distribution Center for Segmentation Antibodies, the Developmental Studies Hybridoma Bank (University of Iowa, USA) for antibodies, and M. Kurusu, E. Piddini, F. Hamaratoglu and the Bloomington Stock Center for fly lines. We are grateful to M. Brauchle for comments on the manuscript and the Unifr Bioimage Facility for assistance with confocal microscopy. This work was funded by Grant 31003A_149499 and Grant CRSII3_136307 from the Swiss National Science Foundation to SGS and by the Swiss University Conference (P-01 BIO BEFRI) to BE.

References

Apitz, H., Salecker, I., 2014. A challenge of numbers and diversity: neurogenesis in the *Drosophila* optic lobe. J. Neurogenet. 28, 233–249.
Apitz, H., Salecker, I., 2015. A region-specific neurogenesis mode requires migratory progenitors in the *Drosophila* visual system. Nat. Neurosci. 18, 46–55.
Bilder, D., 2004. Epithelial polarity and proliferation control: links from the *Drosophila* neoplastic tumor suppressors. Genes Dev. 18, 1909–1925.
Chotard, C., Leung, W., Salecker, I., 2005. *glial cells missing* and *gcm2* cell autonomously regulate both glial and neuronal development in the visual system of *Drosophila*. Neuron 48, 237–251.
Clem, R.J., 2001. Baculoviruses and apoptosis: the good, the bad, and the ugly. Cell Death Differ. 8, 137–143.
Daniel, A., Dumstrei, K., Lengyel, J.A., Hartenstein, V., 1999. The control of cell fate in the embryonic visual system by *atonal*, *tailless* and EGFR signaling. Development 126, 2945–2954.
Egger, B., Boone, J.Q., Stevens, N.R., Brand, A.H., Doe, C.Q., 2007. Regulation of spindle orientation and neural stem cell fate in the *Drosophila* optic lobe. Neural Dev. 2, 1.
Gold, K.S., Brand, A.H., 2014. Optix defines a neuroepithelial compartment in the optic lobe of the *Drosophila* brain. Neural Dev. 9, 18.
Green, P., Hartenstein, A.Y., Hartenstein, V., 1993. The embryonic development of the *Drosophila* visual system. Cell Tissue Res. 273, 583–598.
Gui, H., Li, M.L., Tsai, C.C., 2011. A tale of Tailless. Dev. Neurosci. 33, 1–13.
Hay, B.A., Wolff, T., Rubin, G.M., 1994. Expression of baculovirus P35 prevents cell death in *Drosophila*. Development 120, 2121–2129.
Hofbauer, A., Campos-Ortega, J.A., 1990. Proliferation pattern and early differentiation of the optic lobes in *Drosophila melanogaster*. Roux's Arch. Dev. Biol. 198, 264–274.
Huang, Z., Kunes, S., 1996. Hedgehog, transmitted along retinal axons, triggers neurogenesis in the developing visual centers of the *Drosophila* brain. Cell 86, 411–422.
Huang, Z., Kunes, S., 1998. Signals transmitted along retinal axons in *Drosophila*: Hedgehog signal reception and the cell circuitry of lamina cartridge assembly. Development 125, 3753–3764.
Islam, M.M., Zhang, C.L., 2015. TLX: A master regulator for neural stem cell maintenance and neurogenesis. Biochim. Biophys. Acta 1849, 210–216.
Kosman, D., Small, S., Reinitz, J., 1998. Rapid preparation of a panel of polyclonal antibodies to *Drosophila* segmentation proteins. Dev. Genes Evol. 208, 290–294.
Li, W., Sun, G., Yang, S., Qu, Q., Nakashima, K., Shi, Y., 2008. Nuclear receptor TLX regulates cell cycle progression in neural stem cells of the developing brain. Mol. Endocrinol. 22, 56–64.
Li, X., Erclik, T., Bertet, C., Chen, Z., Voutev, R., Venkatesh, S., Morante, J., Celik, A., Desplan, C., 2013. Temporal patterning of *Drosophila* medulla neuroblasts controls neural fates. Nature 498, 456–462.
Lin, S., Huang, Y., Lee, T., 2009. Nuclear receptor unfulfilled regulates axonal guidance and cell identity of *Drosophila* mushroom body neurons. PloS One 4, e8392.
Manseau, L., Baradaran, A., Brower, D., Budhu, A., Elefant, F., Phan, H., Philp, A.V., Yang, M., Glover, D., Kaiser, K., Palter, K., Selleck, S., 1997. GAL4 enhancer traps expressed in the embryo, larval brain, imaginal discs, and ovary of *Drosophila*. Dev. Dyn. 209, 310–322.
Mardon, G., Solomon, N.M., Rubin, G.M., 1994. *dachshund* encodes a nuclear protein required for normal eye and leg development in *Drosophila*. Development 120, 3473–3486.
Miyawaki, T., Uemura, A., Dezawa, M., Yu, R.T., Ide, C., Nishikawa, S., Honda, Y., Tanabe, Y., Tanabe, T., 2004. Tlx, an orphan nuclear receptor, regulates cell numbers and astrocyte development in the developing retina. J. Neurosci. 24, 8124–8134.
Pereanu, W., Shy, D., Hartenstein, V., 2005. Morphogenesis and proliferation of the larval brain glia in *Drosophila*. Dev. Biol. 283, 191–203.
Perruchoud, B., Egger, B., 2014. Immunofluorescent labeling of neural stem cells in the *Drosophila* optic lobe. Methods Mol. Biol. 1082, 71–78.
Pineiro, C., Lopes, C.S., Casares, F., 2014. A conserved transcriptional network

regulates lamina development in the *Drosophila* visual system. Development 141, 2838–2847.
Roy, K., Kuznicki, K., Wu, Q., Sun, Z., Bock, D., Schutz, G., Vranich, N., Monaghan, A.P., 2004. The Tlx gene regulates the timing of neurogenesis in the cortex. J. Neurosci. 24, 8333–8345.
Rudolph, K.M., Liaw, G.J., Daniel, A., Green, P., Courey, A.J., Hartenstein, V., Lengyel, J. A., 1997. Complex regulatory region mediating *tailless* expression in early embryonic patterning and brain development. Development 124, 4297–4308.
Sanes, J.R., Zipursky, S.L., 2010. Design principles of insect and vertebrate visual systems. Neuron 66, 15–36.
Selleck, S.B., Gonzalez, C., Glover, D.M., White, K., 1992. Regulation of the G1-S transition in postembryonic neuronal precursors by axon ingrowth. Nature 355, 253–255.
Sen, A., Nagy-Zsver-Vadas, Z., Krahn, M.P., 2012. *Drosophila* PATJ supports adherens junction stability by modulating Myosin light chain activity. J. Cell Biol. 199, 685–698.
Sprecher, S.G., Pichaud, F., Desplan, C., 2007. Adult and larval photoreceptors use different mechanisms to specify the same Rhodopsin fates. Genes Dev. 21, 2182–2195.
Tepass, U., 2012. The apical polarity protein network in *Drosophila* epithelial cells: regulation of polarity, junctions, morphogenesis, cell growth, and survival. Annu. Rev. Cell Dev. Biol. 28, 655–685.
Ting, C.Y., Lee, C.H., 2007. Visual circuit development in *Drosophila*. Curr. Opin. Neurobiol. 17, 65–72.
Venken, K.J., Carlson, J.W., Schulze, K.L., Pan, H., He, Y., Spokony, R., Wan, K.H., Koriabine, M., de Jong, P.J., White, K.P., Bellen, H.J., Hoskins, R.A., 2009. Versatile P[acman] BAC libraries for transgenesis studies in *Drosophila melanogaster*. Nat. Methods 6, 431–434.
Yasugi, T., Sugie, A., Umetsu, D., Tabata, T., 2010. Coordinated sequential action of EGFR and Notch signaling pathways regulates proneural wave progression in the *Drosophila* optic lobe. Development 137, 3193–3203.
Yasugi, T., Umetsu, D., Murakami, S., Sato, M., Tabata, T., 2008. *Drosophila* optic lobe neuroblasts triggered by a wave of proneural gene expression that is negatively regulated by JAK/STAT. Development 135, 1471–1480.
Younossi-Hartenstein, A., Green, P., Liaw, G.J., Rudolph, K., Lengyel, J., Hartenstein, V., 1997. Control of early neurogenesis of the *Drosophila* brain by the head gap genes *tll*, *otd*, *ems*, and *btd*. Dev. Biol. 182, 270–283.
Zhang, C.L., Zou, Y., Yu, R.T., Gage, F.H., Evans, R.M., 2006. Nuclear receptor TLX prevents retinal dystrophy and recruits the corepressor atrophin1. Genes Dev. 20, 1308–1320.